

Acetylacetonate bis(thiosemicarbazone) complexes of copper and nickel: towards new copper radiopharmaceuticals

Andrew R. Cowley,^a Jonathan R. Dilworth,^{*b} Paul S. Donnelly,^b Antony D. Gee^c and Julia M. Heslop^b

^a Chemical Crystallography, Laboratory and University of Oxford, 12 Mansfield Road, Oxford, UK OX1 3TA

^b Chemistry Research Laboratory, University of Oxford, 12 Mansfield Road, Oxford, UK OX1 3TA. E-mail: jon.dilworth@chem.ox.ac.uk

^c Clinical Research Unit, GlaxoSmithKline, Translational Medicine and Technologies, ACCI and Addenbrookes Hospital, Hills Road, Cambridge, UK CB2 2GG

Received 29th April 2004, Accepted 30th June 2004

First published as an Advance Article on the web 22nd July 2004

A series of copper(II) and nickel(II) 1,3-bis(thiosemicarbazonato) complexes have been synthesised by the reaction of the metal acetates with pyrazoline proligands. In each case the complexes have an overall neutral charge with a dianionic ligand. The copper 1,3-bis(4-methyl-3-thiosemicarbazonato) complex has been characterised by X-ray crystallography, which shows the copper is in an essentially square-planar symmetric N₂S₂ environment. The nickel 1,3-bis(4-methyl-3-thiosemicarbazonato) and nickel 1,3-bis(4-phenyl-3-thiosemicarbazonato) complexes have been characterised by X-ray crystallography and show that in these cases the nickel is in a distorted square-planar environment, but the bonding mode of the ligands is unusual; the nickel binds to one of the aza-methinic nitrogen atoms and one hydrazinic nitrogen, creating one five-membered N–N–C–S–Ni chelate ring and one four-membered N–C–S–Ni chelate ring. Interestingly, the X-ray structure of the ethyl analogue {1,3-bis(4-ethyl-3-thiosemicarbazonato)nickel(II)} shows that in this case the nickel is symmetrically coordinated in the usual manner. The nickel complexes are diamagnetic and the different coordination modes are confirmed in solution by NMR spectroscopy. The complexes are susceptible to oxidation in air and a nickel complex, in which the central methylene carbon has been oxidised, has been characterised by X-ray crystallography and NMR spectroscopy. Electrochemical measurements show that the copper complexes undergo a reversible one-electron reduction at biologically accessible potentials.

Introduction

Thiosemicarbazones are of great pharmacological interest since they show a broad spectrum of biological activity including antitumour, antibacterial, antimalarial and antifungal activities.¹ Moreover, metal complexes of thiosemicarbazones often display enhanced activities when compared to the uncomplexed thiosemicarbazones. Copper complexes of bis(thiosemicarbazones) have been investigated for use as anti-cancer chemotherapeutic agents^{2,3} and as superoxide dismutase-like radical scavengers.⁴ It is, however, their use as delivery agents for radioactive copper in new copper based radiopharmaceuticals and the hypoxic selectivity of certain copper bis(thiosemicarbazonato) complexes that has created much recent interest.^{5–11} Hypoxia (low oxygen concentrations) is often associated with tumours and heart disease and can affect the outcome of anti-cancer treatments. This means it is of great clinical utility to develop systems that allow the ‘non-invasive’ imaging of hypoxia with a suitable radiopharmaceutical.¹² Copper radionuclides are of considerable interest in the development of new radiopharmaceuticals as they include isotopes that have both PET imaging and therapeutic potential.¹³

The cell uptake and retention characteristics of copper bis(thiosemicarbazonato) complexes derived from 1,2-diones is dependent on the nature of the ‘backbone’ substituents on the ligand.⁶ The radioactive copper complex [⁶⁴Cu(ATSM)] (ligand structures; Fig. 1) shows rapid uptake and washout in normal tissues but is selectively trapped in hypoxic heart and tumour tissue; it is therefore referred to as ‘hypoxia selective’.¹⁰ Other complexes, such as [Cu(GTS)] and [Cu(PTSM)] (Fig. 1), are non-selectively trapped in all cells, which leads to alternative uses. For example, [Cu(PTSM)] has shown great potential as a non-selective blood perfusion tracer.¹⁴

In the case of the hypoxia-selective complex [Cu(ATSM)], the trapping in hypoxic cells is believed to occur *via* reduction of the copper(II) complex by intracellular reducing agents to give a stable

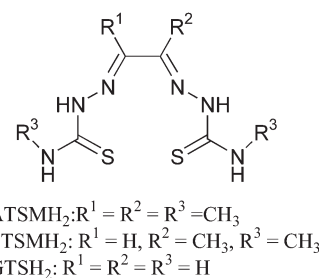


Fig. 1 Bis(thiosemicarbazone) ligands and abbreviations.

protonated Cu(I) species, which is trapped inside the cell.^{10,11} In normal oxic cells, this Cu(I) complex is rapidly oxidised back to the original neutral Cu(II) complex, which quickly washes out of the cell. In the case of the non-selective copper complex [Cu(GTS)], which shows high cell uptake independent of oxygen concentration, it is believed that once the Cu(II) complex enters the cell, it is reduced to Cu(I) and then dissociates from the ligand. The ‘free’ copper is then sequestered by intra-cellular ligands and irreversibly trapped inside the cell.¹⁵

The marked dependence of the nature of the backbone on the specificity of copper complexes of bis(thiosemicarbazones) led us to investigate further bis(thiosemicarbazone) proligands with extended, three-carbon backbones as ligands for the development of new copper radiopharmaceuticals (Fig. 2). It was hoped that these larger ligands would better accommodate both Cu(I) and Cu(II). A cationic nickel complex of R = H has been structurally characterised¹⁶ and the copper complex of L¹ has been recently reported but was not structurally characterised.¹⁷ Whilst complexes of L¹ with technetium have been investigated as potential imaging agents,^{18,19} there is some doubt as to the nature of the species formed.²⁰ To our knowledge nobody has attempted to study the radiocopper complexes of these proligands.

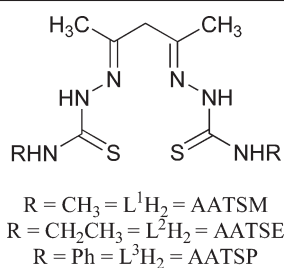


Fig. 2 Bis(thiosemicarbazone) proligands and abbreviations.

This paper describes the synthesis and full characterisation of a series of (bis)thiosemicarbazone proligands derived from 1,3-diketones, their copper complexes, including a study of their redox properties, and an evaluation of their potential to act as radiopharmaceuticals. In an attempt to characterise further the coordination behaviour of these ligands, we have also investigated their nickel complexes.

Results and discussion

Synthesis

The synthesis of bis(thiosemicarbazones) by the reaction of thiosemicarbazides with 2,4-pentanedione is complicated by cyclisation reactions, which result in the isolated product being in the pyrazoline form.²⁰ Fortunately, it has been shown recently that these pyrazolines undergo ring opening back to a bis(thiosemicarbazone) in the presence of certain transition metal ions, resulting in the formation of the bis(thiosemicarbazonato) metal complex.¹⁷ It has been highlighted recently that this has led to confusion in the literature, and some misinterpretation of the nature of materials isolated from the reaction of thiosemicarbazides directly with 2,4-pentanedione.²⁰

The pyrazoline proligands were readily synthesised and isolated by literature procedures, which involve the reaction in the presence of acid of two equivalents of thiosemicarbazide with 1,2-bis(1-methyl-3-oxobutylideneamino)ethane (**1**), which is isolated from the reaction of 2,5-pentanedione with 1,2-ethanediamine (Fig. 3).²¹ An X-ray crystal structure of the molecule (H_2L^2) isolated from the reaction of 4-ethyl-3-thiosemicarbazide with **1** is shown in Fig. 4 and confirms the molecule is in the pyrazoline form.

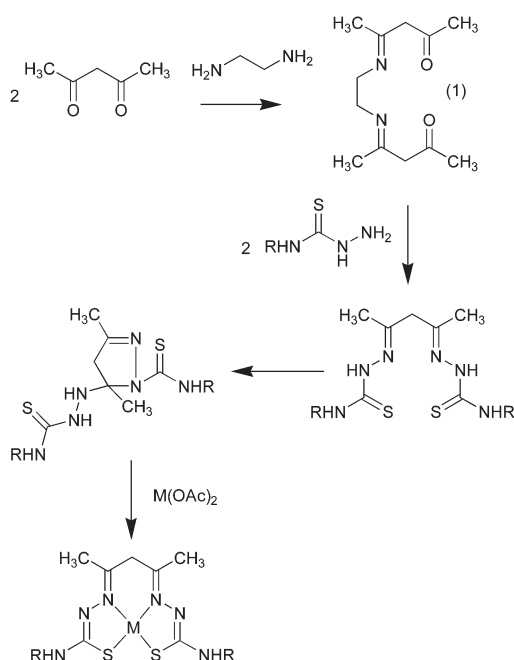


Fig. 3 Reaction scheme for the synthesis of $[\text{M}(\text{AATS})]$ complexes.

The structure is similar to the methyl analogue which has been reported recently.^{17,20} One of the hydrazine H atoms forms an intramolecular hydrogen bond to one of the S atoms ($\text{N}(3)\cdots\text{S}(1)$ 3.1715(19) Å). The second hydrazine H atom and one of the thio-

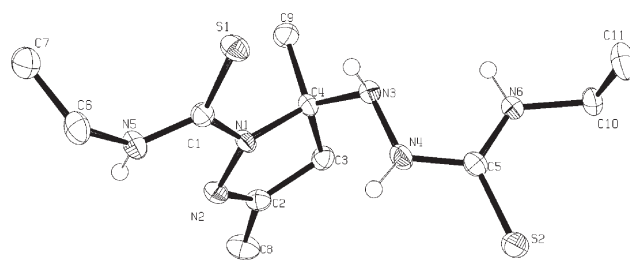


Fig. 4 An ORTEP representation of ethylthiosemicarbazido-pyrazoline (H_2L^2).

amide H atoms link the molecules to form dimers ($\text{N}(4)\cdots\text{N}(2)'$ 3.194(2), $\text{N}(5)\cdots\text{S}(2)'$ 3.3365(18) Å, a symmetry operator generating acceptor atoms $-x, 1-y, 1-z$). The remaining NH groups form longer $\text{N}\cdots\text{S}$ hydrogen bonds that link the dimers to form infinite chains running parallel to the crystallographic c axis ($\text{N}(6)\cdots\text{S}(1)''$ 3.5427(18) Å, a symmetry operator generating acceptor $-x, 1-y, -z$).

Whilst this method worked well for the synthesis of the methyl and ethyl analogues (H_2L^1 and H_2L^2) in their pyrazoline form, problems were encountered in synthesising the phenyl analogue (H_2L^3). In this case, the elemental analysis of the isolated bulk material was not consistent with H_2L^3 in the pyrazoline form, although it was of sufficient purity to make metal complexes that gave satisfactory mass spectra and, in the case of the nickel complex crystals suitable for X-ray crystallography. An attempt to purify crude H_2L^3 by recrystallisation from ethanol gave colourless crystals that were shown by X-ray crystallography, mass spectroscopy and NMR to be *N,N*-diphenyl[1,3,4]thiadiazole-2,5-diamine (**2**) (Fig. 5), which proved to be a major contaminant in the product. The synthesis of this compound has been reported directly from 4-phenylthiosemicarbazide in the presence of sulfuric acid.²² Pure H_2L^3 in the pyrazoline form could be obtained in moderate yield (58%) by performing the synthesis in the absence of acid.

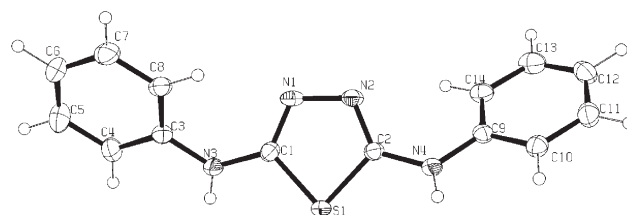


Fig. 5 An ORTEP representation of *N,N*-diphenyl[1,3,4]thiadiazole-2,5-diamine (**2**).

The copper complexes of the three-carbon backbone ligands were prepared by reaction of the pyrazoline proligands with $\text{Cu}(\text{CH}_3\text{CO}_2)_2$ in methanol under an atmosphere of nitrogen and copper complexes of $\text{L}^1\text{--L}^3$ were isolated in this manner. The complexes precipitated from the reaction mixture and could be readily isolated by filtration. An ORTEP representation of the complex obtained by the reaction of H_2L^1 with copper acetate is shown in Fig. 6 (crystallographic data appears in Table 1 and selected bond lengths for the complexes are given in Table 2). The neutral complex contains a square-planar copper atom coordinated to each of the sulfur and azomethinic nitrogen atoms. The Cu–S bond distances of 2.2469(5) and 2.2335(5) Å are very similar to copper(II) thiolate bond distances found in “simple” N_2S_2 chelates and the hypoxia selective radiopharmaceutical $[\text{Cu}(\text{ATSM})]$ (Fig. 1).^{11,23} The Cu–N bond distances of 1.9737(16) and 1.9893(16) Å are also similar to the Cu–N bond distances in $[\text{Cu}(\text{ATSM})]$. Although the bond distances are similar to $[\text{Cu}(\text{ATSM})]$, there are significant differences in the bond angles around the copper, which are closer to the ideal for a square-planar system in the complex with the larger ligand, $[\text{Cu}(\text{L}^1)]$. The S–Cu–N bond angles are 86.79(5) and 85.60(5)°, whereas in $[\text{Cu}(\text{ATSM})]$ the S–Cu–N bond angles average is 85.17°. Bigger differences are evident in the N–Cu–N angle, which is 96.10(7)° in $[\text{Cu}(\text{L}^1)]$ compared with an average of 80.60° in $[\text{Cu}(\text{ATSM})]$, and the S–Cu–S angle, which is 91.728(19)° in $[\text{Cu}(\text{L}^1)]$ compared with

Table 1 Crystallographic data

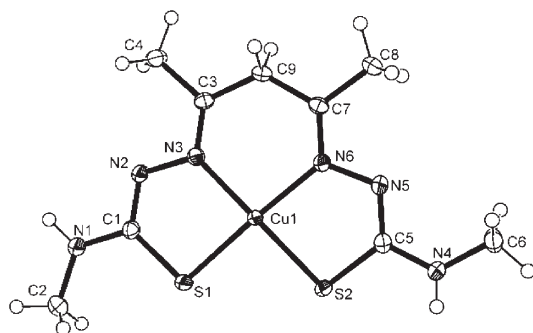
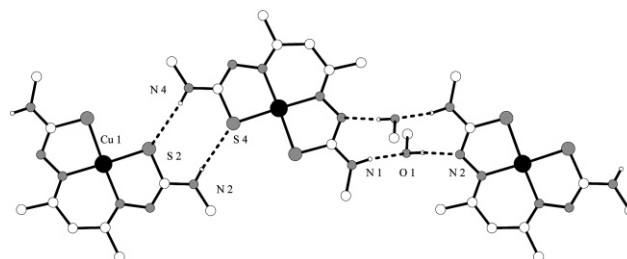
Crystal identification	2	H ₂ L ²	[Cu(L ¹)]	[Ni(L ¹)]	[Ni(L ³)]	[Ni(L ² O)]
Chemical formula	C ₁₄ H ₁₂ N ₄ S	C ₁₁ H ₂₂ N ₆ S ₂	C ₁₀ H ₂₀ CuN ₆ OS ₂	C ₉ H ₁₆ N ₆ NiS ₂	C ₁₉ H ₂₀ N ₆ NiS ₂	C ₁₁ H ₁₈ N ₆ NiOS ₂
<i>M</i>	268.34	302.46	367.97	331.10	455.24	373.14
Crystal system	Monoclinic	Triclinic	Triclinic	Orthorhombic	Monoclinic	Monoclinic
Space group	<i>Pc</i>	<i>P</i> $\bar{1}$	<i>P</i> $\bar{1}$	<i>Pcba</i>	<i>P2₁/c</i>	<i>P2₁/c</i>
<i>a</i> /Å	11.0953(2)	8.2326(3)	7.6332(2)	8.2450(2)	7.6882(2)	20.5059(4)
<i>b</i> /Å	7.0982(2)	9.8339(3)	8.2419(2)	17.2004(2)	20.5594(5)	8.1622(2)
<i>c</i> /Å	8.5325(2)	10.0725(4)	12.8765(3)	19.5299(3)	12.7497(4)	19.1350(4)
<i>a</i> /°	90	106.4508(17)	72.6838(9)	90	90	90
<i>β</i> /°	104.4051(9)	95.7000(17)	85.4540(9)	90	105.6694(11)	104.6903(9)
<i>γ</i> /°	90	91.7108(13)	85.3228(8)	90	90	90
<i>V</i> /Å ³	650.83(3)	776.77(5)	769.51(3)	2769.68(9)	1940.38(9)	3097.99(12)
<i>Z</i>	2	2	2	8	4	8
<i>R</i> _{int}	0.055	0.043	0.029	0.032	0.047	0.050
<i>wR</i>	0.0480	0.0374	0.0351	0.0316	0.0310	0.0335
<i>ρ</i> _{max/min} /e Å ⁻³	-0.29, 0.45	-0.24, 0.19	-0.36, 0.34	-0.32, 0.36	-0.35, 0.25	-0.40, 0.41

Table 2 Selected bond distances (Å) in the complexes

	[Cu(L ¹)]	[Ni(L ¹)]	[Ni(L ³)]	[Ni(L ² O)]
Cu(1)–N(3)	1.9737(16)	Ni(1)–N(2)	1.9026(15)	Ni(1)–N(2)
Cu(1)–N(6)	1.9893(16)	Ni(1)–N(4)	1.9065(15)	Ni(1)–N(3)
Cu(1)–S(1)	2.2469(5)	Ni(1)–S(1)	2.1675(5)	Ni(1)–S(1)
Cu(1)–S(2)	2.2335(5)	Ni(1)–S(2)	2.2279(5)	Ni(1)–S(2)
			Ni(1)–N(2)	1.8999(19)
			Ni(1)–N(4)	1.908(2)
			Ni(1)–S(1)	2.1464(7)
			Ni(1)–S(2)	2.2210(7)
			Ni(1)–N(2)	1.905(2)
			Ni(1)–N(3)	1.904(3)
			Ni(1)–S(1)	2.1505(9)
			Ni(1)–S(2)	2.1512(8)

an average of 109.22° in [Cu(ATSM)].²³ This suggests that the larger ligand, L¹, is in general a better fit for copper(II) than the smaller ATSM ligand. The thiosemicarbazonato ligand is dianionic and all the non-hydrogen atoms are approximately coplanar (rms deviation from best plane 0.09 Å). This results in considerable strain at the methylene C atom, as shown by the abnormally large value of the C(3)–C(9)–C(4) angle (126.15(16)°). The bond distances within the ligand show extensive conjugation within the ligand but the resonance form depicted in Fig. 3, in which the ligand is dianionic, predominates. It is interesting to note that this resonance form is preferred to one in which the central CH₂ group is deprotonated, resulting in a conjugated ligand with an overall monoanionic charge. The C–S bond lengths of 1.737(2) and 1.751(2) Å are similar to the analogous bond distances in [Cu(ATSM)] and consistent with a bond order greater than 1 but less than 1.5. There are also similarities between [Cu(ATSM)] and [Cu(L¹)] in the carbon to nitrogen bond distances in the SN–C=N fragments and the N–C=N fragments. In [Cu(L¹)] the SN–C=N bond distances are 1.320(3) and 1.310(3) Å; the N–C=N bond distances are 1.293(2) and 1.292(3) Å. These distances are indicative of a bond order greater than 1.5 but less than 2. The greatest difference between [Cu(ATSM)] and [Cu(L¹)] arises in the N–N bond distance, which is significantly shorter in [Cu(ATSM)] (average value 1.369 Å) than it is in **1** (1.397(2) and 1.402(2) Å).²³ This relatively long value is indicative of a reduction in the delocalisation of electron density. Perhaps this explains, at least in part, why we have found complexes of the type [Cu(L¹)] more susceptible to protonation at the hydrazinic nitrogen (N5, N2) than complexes of the ATSM type. This could be of importance for any biological selectivity.

As is the case for the two-carbon backbone copper(II) bis(thiosemicarbazone) radiopharmaceuticals,²³ the crystal

**Fig. 6** An ORTEP representation of [Cu(L¹)].**Fig. 7** Diagram of the hydrogen bonding array in [Cu(L³)].

structure of the complex reveals an extensive hydrogen bonding array (Fig. 7).

The nature of the hydrogen bonding interaction within these compounds could be of some relevance to the biological activity through possible interactions with nucleoside bases and peptide bonds. One of the NH groups forms a hydrogen bond to the O atom of a nearby solvent (N(1)···O(1) 2.824(2) Å, symmetry operator 1 – *x*, 2 – *y*, –*z*). The second NH group forms a hydrogen bond to a S atom of a second molecule of complex (N(4)···S(2) 3.3956(19) Å, symmetry operator –*x*, –*y*, 1 – *z*). The solvent OH forms a hydrogen bond to a N atom in the same asymmetric unit (O(1)···N(2) 2.819(2) Å). These hydrogen bonds link the complexes and solvents to form infinite chains.

The reaction of Ni(CH₃CO₂)₂ with the proligands in their pyrazoline form also resulted in ring opening of the proligand to allow the isolation of the nickel complexes of L¹–L³. In the case of L¹ and L³ green and green–brown solids were isolated from the reaction mixture respectively, but interestingly, the product from the reaction of L² was pink. The ES-MS all show peaks corresponding to [Ni(L¹⁻³) + H⁺].

The nickel complex of L¹ was isolated as crystals that exhibit pronounced pleochroism; when viewed along the *b* axis they appear very dark green, but when viewed along the *c* axis they appear red–brown. A representation of the X-ray structure is shown in Fig. 8.

Like the copper complex, the nickel complex is essentially square planar with N₂S₂ coordination, but somewhat surprisingly the bonding mode of the ligands is quite different, with the nickel binding to one azamethinic nitrogen and one hydrazinic nitrogen, creating one five-membered N–Ni–S chelate ring and one four-membered N–Ni–S chelate ring. Whilst this binding mode is known for thiosemicarbazones, it is rare.²⁴ The presence of the four-membered chelate ring does introduce a significant amount of distortion and the bond angles around the nickel are much further away from the ideal

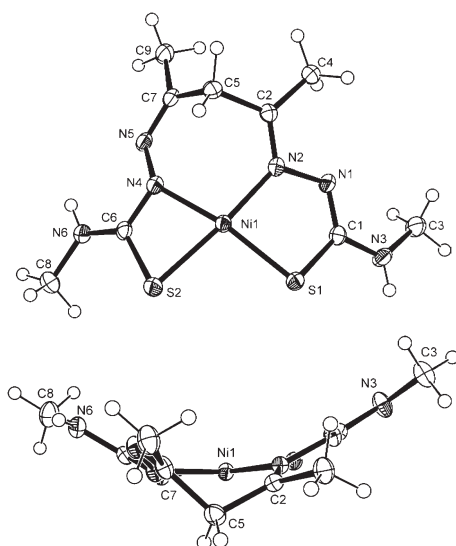


Fig. 8 An ORTEP representation of $[\text{Ni}(\text{L}^1)]$.

value than in a similar nickel complex (where $\text{R} = \text{NH}_2$), which is symmetrically bound with two five-membered N–Ni–S chelate rings.¹⁶ The N4–Ni–S2 bond angle in the four-membered chelate is $73.94(5)^\circ$, whilst the N2–Ni–S1 bond angle of the five-membered ring is $86.98(5)^\circ$. Despite these distortions, the geometry of the nickel atom is still approximately planar with the rms deviation of the Ni, S and coordinated nitrogen atoms from the best plane being 0.054 \AA . The Ni–S bond lengths are similar to other compounds with N–S thiolate coordination.²⁵ Once again, the ligand is doubly deprotonated, but, in this case, much less planar than the copper analogue.

The conformation of the ligand generates a ‘bowl-like’ shape (see Fig. 8) with the CH_2 of the backbone folded below the plane containing the nickel. This conformation is perhaps facilitated by the non-symmetrical coordination that reduces the strain within the C– CH_2 –C backbone when compared to the copper complex. It appears as if the ligand consists of two nearly planar sections, which are joined at the ‘backbone’ CH_2 with a C2–C5–C7 bond angle of $109.46(14)^\circ$. The bond lengths within the ligand still indicate extensive delocalisation throughout the ligand but the resonance form depicted in Fig. 3 still predominates.

Crystals of the nickel complex of the phenyl substituted ligand, L^3 , suitable for X-ray studies, were grown by slow evaporation of a dichloromethane solution of the complex. A representation of the structure is depicted in Fig. 9. Once again, the metal atom coordinates to the bis(thiosemicarbazone) ligand in a non-symmetrical fashion, with an approximately square-planar nickel and a 4–7–5 chelate system. The Ni–S and Ni–N bond lengths are similar to the previous example, $[\text{Ni}(\text{L}^1)]$, as are the bond angles. The ligand is doubly deprotonated with a similar conformation to the methyl analogue, although in this case there is slightly less deviation from planarity at the C– CH_2 –C ‘backbone’ of the ligand, with a C2–C3–C4 bond angle of $114.2(2)^\circ$. Once again, the ‘bowl-like’ conformation of the ligand reduces the strain within the backbone.

NMR studies

The d^8 square-planar nickel complexes are all diamagnetic and give well resolved NMR spectra, which confirm the nature of the binding. The ^1H NMR spectrum of $[\text{Ni}(\text{L}^1)]^+$ shows signals for the CH_3 groups (δ 1.91 and 2.16 ppm) and a multiplet corresponding to the two NHCH_3 resonances (δ 2.63 ppm). The two NH resonances are split into multiplets by the neighbouring CH_3 groups and are clearly distinct, occurring at δ 6.85 and 8.00 ppm, respectively. The ^{13}C NMR spectrum is also consistent with non-symmetric binding, with two methyl resonances corresponding to the ‘backbone’ CH_3 groups (δ 21.5 and 22.9 ppm) and two resonances corresponding to the terminal CH_3 groups (δ 27.3 and 30.8 ppm). A HSQC experiment has shown that the central methylene signal is partially obscured by

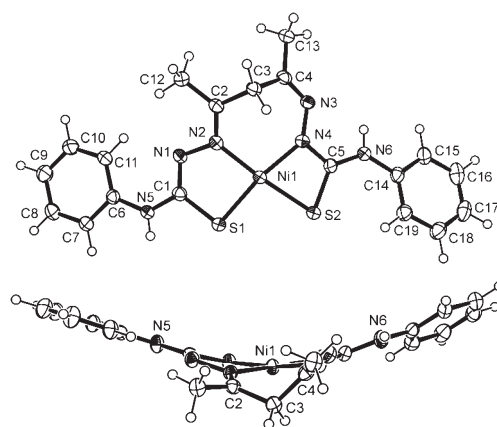


Fig. 9 An ORTEP representation of $[\text{Ni}(\text{L}^3)]$.

the d_6 -DMSO signal. There are also two resonances corresponding to the imino carbons (δ 151.1 and 157.8 ppm) and the C–S groups (δ 173.3 and 176.2 ppm).

In the case of the N-phenyl substituted ligand, L^3 , the ^1H NMR spectrum also shows the complex is doubly deprotonated at the hydrazinic nitrogens and that the nickel is non-symmetrically bound. There are two signals for the CH_3 groups (δ 2.09 and 2.33 ppm), a series of overlapping multiplets corresponding to the aromatic resonances (δ 6.90–7.58 ppm) and two NH resonances (δ 9.42 and 10.18 ppm). The ^{13}C NMR spectrum has two methyl resonances (δ 23.0 and 23.6 ppm) and a series of aromatic resonances (δ 118.3–141.0 ppm). There are two resonances corresponding to the imino carbons (δ 153.8 and 162.3 ppm) and the C–S groups (δ 169.4 and 173.2 ppm). These spectra confirm that in these cases the solid state structures correspond with those in solution.

Interestingly, the ^1H and ^{13}C NMR spectra of the pink solid, $[\text{Ni}(\text{L}^2)]^+$, indicate that in this case the nickel is symmetrically coordinated. The ^1H NMR spectrum has one signal corresponding to the CH_3 groups (δ 2.11 ppm) and two multiplets corresponding to the terminal NHCH_2CH_3 groups (δ 3.12 and 1.03 ppm, respectively). The NH resonance is split into a multiplet by the neighbouring CH_2CH_3 groups and occurs at δ 6.94 ppm. The ^{13}C NMR spectrum has a single resonance corresponding to the ‘backbone’ methyl groups (δ 20.4 ppm) and a signal corresponding to the terminal methyl groups of the ethylene moieties (δ 14.4 ppm). A HSQC experiment has shown that the NHCH_2 signal is partially obscured by the d_6 -DMSO signal. There are single resonances corresponding to the imino carbons (δ 156.9 ppm) and the C–S groups (δ 171.0 ppm).

Oxidation of the complexes

Recently Durrant and co-workers reported that the ligand in $[\text{Cu}(\text{L}^1)]$ is susceptible to oxidation in air. They suggested that the oxidation involved the addition of a single oxygen atom to the methylene backbone with a concomitant loss of two hydrogen atoms (Fig. 10).¹⁷

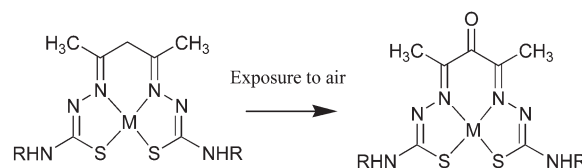


Fig. 10 Oxidative formation of complexes $[\text{M}(\text{L}^{1-3}\text{O})]$.

The electronic spectra of $[\text{Cu}(\text{L}^1)]$ prepared under nitrogen has a weak intensity d–d band at 778 nm. There is also a weak intensity band at 555 nm and medium to high intensity bands at 417, 318 and 293 nm which are assigned to ligand to metal charge transfer and intraligand transitions. On exposure to air, the spectrum gradually changes over time, but rapid oxidation, as previously reported,¹⁷ was not observed. After the sample had been exposed to air for 15 h

the electronic spectrum showed peaks that have been attributed to the oxidised complex (483 and 378 nm) but also retains a band at 417 nm which has been attributed to the original 'non-oxidised' product, $[\text{Cu}(\text{L}^1)]^+$.¹⁷ This suggests that the after a sample of the compound has been exposed to air for 15 h a mixture of the oxidised and non-oxidised copper complexes is present.

If the copper acetate is reacted with the proligand H_2L^1 in ethanol, but this time in an aerobic environment (rather than under nitrogen), a brown solid is obtained. The electronic spectrum of this material suggests that it contains a mixture of $[\text{Cu}(\text{L}^1)]$ and its oxidised product. The ES-MS of this material also shows a peak at $m/z = 335$, corresponding to $[\text{Cu}(\text{L}^1) + \text{H}^+]$ (copper in the +III oxidation state),²⁶ and a peak at $m/z = 350$, which corresponds to the oxidised product. HPLC analysis (C18 reverse phase column with ammonium acetate–acetonitrile gradient elution) of the solid dissolved in DMSO revealed two peaks with elution times of 15.3 and 16.0 min. The two peaks presumably correspond to non-oxidised and oxidised product.

The crystals used for the X-ray studies of $[\text{Cu}(\text{L}^1)]$ (Fig. 6) were grown under an atmosphere of nitrogen. The restrictions of the square-planar coordination about the copper results in considerable strain at the methylene C atom, as shown by the abnormally large value of the C(3)–C(9)–C(4) angle ($126.15(16)^\circ$). The oxidation of the ligand may actually be a consequence of the ligand trying to reduce this strain, and may involve deprotonation of the methylene carbon followed by electrophilic attack. Addition of Na_2CO_3 to a solution, which contained a mixture of $[\text{Cu}(\text{L}^1)]$ and the oxidised complex, resulted in increasing the intensity of a band at 363 nm in the UV/vis spectrum which is attributed to the oxidised complex.

The X-ray structures of the green/brown crystals of $[\text{Ni}(\text{L}^1)]$ and $[\text{Ni}(\text{L}^3)]$, that display the non-symmetric coordination environment of the metal, show that the ligand is in a 'bowl-like shape' with reduced strain at the methylene carbon. Perhaps this explains why these nickel complexes are more resistant to oxidation, the crystals of $[\text{Ni}(\text{L}^3)]$ were grown *via* evaporation of a dichloromethane solution under an aerial environment.

As mentioned previously, the nickel complex of the ethyl ligand L^2H_2 was isolated as a pink solid in which the nickel was shown by NMR to be symmetrically coordinated, $[\text{Ni}(\text{L}^2)]$. An attempt to grow crystals suitable for X-ray studies from a methanolic solution exposed to air resulted in the isolation of dark brown crystals which were shown by X-ray crystallography to be the oxidised product, $[\text{Ni}(\text{L}^2\text{O})]$ (Fig. 11).

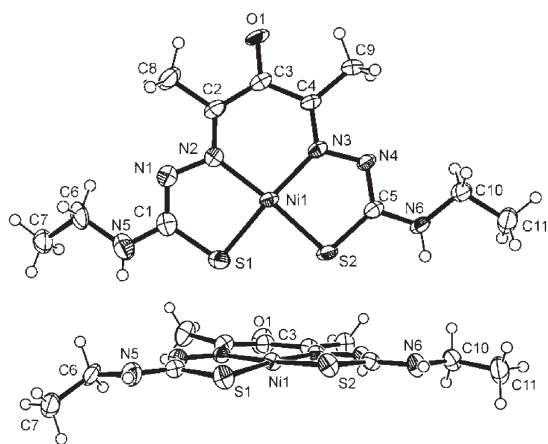


Fig. 11 An ORTEP representation of $[\text{Ni}(\text{L}^2\text{O})]$.

In this case, the ligand has indeed been oxidised at the methylene carbon, to give a ketone (bis)thiosemicarbazone. Although there has been some earlier suggestions of this oxidative degradation,^{17,27} this is the first structurally characterised example. The asymmetric unit contains two distinct molecules, neither of which has any crystallographic symmetry. The complex is essentially square planar with the ligand coordinating in a symmetric manner. Despite the different coordination mode and oxidised ligand, the Ni–N and Ni–S bond lengths and angles are similar to the two previous examples. The

ligand is doubly deprotonated with approximately planar geometry with the exception of its ethyl groups.

One of the molecules forms hydrogen bonds with both NH groups ($\text{N}(5)\cdots\text{O}(2)$ 3.141(5) Å, $\text{N}(6)\cdots\text{O}(1)$ 2.938(3) Å, symmetry operator of acceptor $x, 1/2 - y, 1/2 + z$) (Fig. 12). The second molecule does not act as a hydrogen-bond donor. The hydrogen bonds link the complexes to form infinite chains running parallel to the crystallographic c axis.

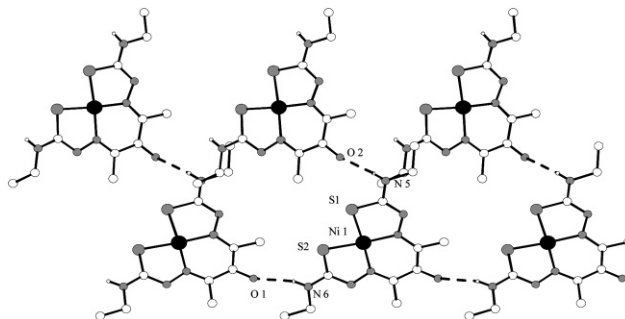


Fig. 12 Diagram of the hydrogen bonding array in $[\text{Ni}(\text{L}^2\text{O})]$.

NMR analysis of the crystals used for the X-ray studies confirmed that the oxidised product could be identified by its NMR spectra with loss of the peaks attributed to the methylene 'backbone' in the ^1H NMR and an additional carbonyl peak at δ 181.9 ppm in the ^{13}C NMR spectrum.

Copper(II) and zinc(II) complexes of β -diketiminato ligands, derived from reacting an amine with acetylacetonate, have been demonstrated to undergo a similar oxidation to give ketone diimine derivative under aerobic conditions. In this case the oxidation is assumed to occur *via* a series of steps, which are facilitated by the presence of the metal ion, following addition of dioxygen to the deprotonated methylene carbon.²⁸ Presumably a similar mechanism can be invoked for the oxidation of the metal complexes of bis(thiosemicarbazones) ligands encountered in this work.

Electrochemistry

Structure–activity relationships of copper(II)(bis)thiosemicarbazone radiopharmaceuticals derived from 1,2-diones show a correlation with the reduction potential for the $\text{Cu}(\text{II})/\text{Cu}(\text{I})$ couple and hypoxic cell selectivity.²⁹ The hypoxia selective radiopharmaceutical, $[\text{Cu}(\text{ATSM})]$, undergoes a reversible reduction at $E_{1/2} = -0.62$ V in DMF at a glassy carbon working electrode. The cyclic voltammograms of $[\text{Cu}(\text{L}^1)]$ in DMF with a glassy carbon electrode exhibits a quasi-reversible reduction at $E_{1/2} = -0.37$ V, which was assigned to a $\text{Cu}(\text{II})/\text{Cu}(\text{I})$ process, but also a pre-absorption wave. There was also a broad irreversible oxidation at higher potentials ($E_{\text{ox}} = 0.76$ V), which is presumably due to a ligand based oxidation.

The cyclic voltammetry measurements of the copper complexes, which were prepared in air, were sometimes complicated by the fact that the samples contained mixtures of both the oxidised copper complex and that of the original 'non-oxidised' complex. In these cases two independent reversible reductions could be seen in the cyclic voltammogram. Addition of a small amount of sodium carbonate to these analyte solutions to complete the oxidation resulted in diminution of one of the processes, to give a single reversible process, which was attributed to a reversible one-electron reduction which we attribute to a $\text{Cu}(\text{II})/\text{Cu}(\text{I})$ process (Fig. 13). The 'oxidised' copper complex of L^1 , $[\text{Cu}(\text{L}^1\text{O})]$, has an $E_{1/2} = -0.30$ V (*vs.* SCE) with an anodic to cathodic peak separation of 102 mV (under the same conditions ferrocene had a peak separation of 102 mV); the oxidised complex of L^2 , $[\text{Cu}(\text{L}^2\text{O})]$, has an $E_{1/2} = -0.34$ V with a peak separation of 96 mV. The copper complex of the phenyl substituted ligand, $[\text{Cu}(\text{L}^3\text{O})]$ exhibits a dramatically different $\text{Cu}(\text{II})/\text{Cu}(\text{I})$ reduction potential; the reduction occurs at a potential about 250 mV more positive, ($E_{1/2} = -0.06$ V *vs.* SCE), than the alkyl substituted analogues. It is worth mentioning that the alkyl substituted compounds give red/brown solutions in the DMF

used for electrochemical measurements, whereas the solution of the phenyl derivative, $[\text{Cu}(\text{L}^3\text{O})]$, is dark green. This could suggest that the large shift in the reduction potential is related to some degree of protonation of the complex and that the phenyl substituent dramatically effects the $\text{p}K_{\text{a}}$ of the complex. The cyclic voltammograms of the 'oxidised' complexes, $[\text{Cu}(\text{L}^1\text{-}^3\text{O})]$, all show an irreversible oxidation at higher potentials, which is presumably due to a further ligand based oxidation, which obscures any possible $\text{Cu}(\text{II})/\text{Cu}(\text{I})$ redox processes.

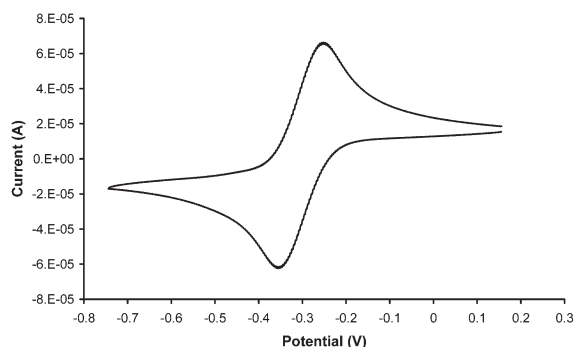


Fig. 13 Cyclic voltammogram of $[\text{Cu}(\text{L}^1\text{O})]$.

Since hypoxic cells are known to be mildly acidic, the measurements were repeated after addition of some aqueous hydrochloric acid to the sample solutions. The resultant voltammograms showed loss of reversibility of the $\text{Cu}(\text{II})/\text{Cu}(\text{I})$ couple. This suggests that in the acidic environment of hypoxic cells reduction is likely to be coupled to protonation as has been suggested for $[\text{Cu}(\text{ATSM})]$.³⁰

Stability studies in human serum

If these complexes are to be used as copper radiopharmaceuticals, it is essential that they are sufficiently stable with respect to loss of metal ion from the chelate in human serum. The perfusion tracer $[\text{Cu}(\text{PTSM})]$ (Fig. 1) was found to be a promising tracer in animals, but problems were encountered in the use of $^{62}\text{Cu}(\text{PTSM})$ at high flow rates in humans. This was attributed to interspecies variability in the binding of $[\text{Cu}(\text{PTSM})]$ to serum albumin. It was shown that $[\text{Cu}(\text{PTSM})]$ had stronger interaction with human serum albumin than it did with dog serum albumin, but that the chelate remains intact in its interaction with the albumin.³¹

$[\text{Cu}(\text{L}^1\text{O})]$ was incubated in human serum at 37 °C for 6 h. Copper(II) acetate and the copper complex of histidine, $[\text{Cu}(\text{hist})_2]$, were also incubated as controls. $[\text{Cu}(\text{hist})_2]$ is known to form a well defined complex with human serum albumin, the primary component of human serum.³² The mixtures were then applied to a Sephadex G-25 PD-10 size exclusion column, which had been previously equilibrated with 0.01 mol L⁻¹ KH_2PO_4 . The column was eluted with phosphate buffer and 2 mL fractions were collected. The high molecular weight proteins rapidly eluted (second fraction) and were identified by monitoring their UV absorbance at 280 nm. The protein fractions were then analysed for copper content by ICP-AES. The protein fractions collected from the human serum that had been incubated with copper(II) acetate and $[\text{Cu}(\text{hist})_2]$ contained 19 and 48% of the total copper concentration added, respectively. In comparison, the protein fraction that was collected from the sample that had been incubated with $[\text{Cu}(\text{L}^1\text{O})]$ analysed as containing negligible amounts of copper. Separation of $[\text{Cu}(\text{L}^1\text{O})]$, from the high molecular weight proteins could be observed visually with the dark brown complex eluting down the column slowly (3rd 2 mL fraction). This suggests $[\text{Cu}(\text{L}^1\text{O})]$ does not relinquish its copper to high molecular weight proteins or bind to human serum albumin after being incubated in human serum at 37 °C for 6 h.

Concluding remarks

The above studies show that the synthesis of bis(thiosemicarbazone) proligands from acetylacetonate is complicated by ring closure reactions, that result in the formation of compounds that

contain a pyrazoline ring. Reaction with either copper or nickel acetate opens the ring to allow the formation of metal complexes. In all the cases reported here, where the metal acetate is used to form the complex, the ligand deprotonates twice to give a dinegative ligand, which is best described as being in the form depicted in Fig. 3. In a related example, in which $\text{Ni}(\text{NO}_3)_2$ was used as the source of metal ion, the X-ray structure shows that the ligand is monoanionic, and deprotonation occurs at the central CH_2 group.¹⁶ The ligands show some flexibility in their binding characteristics, as shown by the nickel complexes that have four-, five- and seven-membered chelate rings and the complexes that display the more expected symmetric 5–6–5 membered chelate ring system. The symmetrically coordinated copper complex reveals considerable strain at the backbone methylene carbon and the complexes are sensitive to oxidative degradation to give keto-bis(thiosemicarbazone) metal complexes, as shown by the structural characterisation of an oxidised nickel complex. This oxidation is accelerated in basic solution. To prevent this oxidation it is essential to prepare the compounds with the rigorous exclusion of air. If the copper complexes are prepared in air, then a mixture of the oxidised and non oxidised products is obtained. The copper complexes show reversible one-electron reductions, which are attributed to a $\text{Cu}(\text{II})/\text{Cu}(\text{I})$ process.

The presence of oxo and non-oxo complexes could explain the presence of two different compounds, as determined by radio-HPLC, in experiments that have attempted to radiolabel H_2L^2 with $^{99\text{m}}\text{Tc}$.^{18,19} All of these complicating factors need to be considered, in these deceptively simple systems, if they are to be used as ligands in radiopharmaceutical preparations. Despite these complications, the copper compounds exhibit good stability in human serum and our preliminary radiolabelling experiments with H_2L^1 and ^{64}Cu show that, under certain conditions, a single copper complex can be synthesised with high radiochemical purity that exhibited high levels of cell uptake.³³ The complexes described here offer the potential to act as more lipophilic variants, with different electrochemistry, and consequently cell uptake characteristics, to the well known copper bis(thiosemicarbazone) radiopharmaceuticals derived from 1,2-diones.

Experimental

General

Elemental and ICP-AES analyses were carried out by the microanalysis service of the department. NMR spectra were recorded on a Varian Mercury VX300 spectrometer using the deuterated solvent signal as an internal reference. Mass spectra were recorded on a Micromass LCT Time of Flight Mass Spectrometer using the electrospray ionisation technique. UV/VIS spectra were recorded on a Cintra 10 UV/VIS spectrometer (solution concentration 2.5×10^{-5} M). Cyclic voltammograms were recorded on a CH instruments Electrochemical Analyser using a platinum working electrode, a platinum counter electrode and a silver pseudo reference electrode. Ferrocene was used as an internal reference which was taken as having an $E_{1/2} = 0.53$ V in DMF vs. SCE. All reagents and other solvents were obtained from standard commercial sources and were used as received.

Syntheses

Synthesis of the ligands **1** and H_2L^{1-3} was based on a procedure described by Durrant and co-workers²¹

1. Pentane-2,4-dione (20 g, 19.98 mmol) was added to ethylenediamine (6 g, 99.83 mmol) in water (150 mL). After 6 h standing, a bulky white solid settled out of solution and was recrystallised from water to give **1** as white feathery needles (12.76 g, 56.89 mmol, 57%).

Synthesis of proligands

H_2L^1 . **1** (3.15 g, 14.04 mmol) and 4-methyl-3-thiosemicarbazide (2.97 g, 28.24 mmol) were added to ethanol (150 mL) and concentrated sulfuric acid (5 drops) was added. The mixture was heated

at reflux under an atmosphere of nitrogen for 3 h and allowed to cool slowly to room temperature. A white precipitate formed which was collected by filtration and washed with diethyl ether to give H_2L^1 as a white powder (2.43 g, 8.85 mmol, 62%) (Found: C, 39.3; H, 6.4; N, 29.9. Calc. for $\text{C}_9\text{H}_{18}\text{N}_6\text{S}_2$: C, 39.4; H, 6.6; N, 30.6%). ^1H NMR (DMSO- d_6): δ 1.73, 3H, s, 5- CH_3 ; 1.95, 3H, s, 3- CH_3 ; 2.79, 2H, d, CH_2 ; 2.85, 3H, d, CH_3N ; 2.89, 3H, d, CH_3N ; 6.40, 1H, s, 5-NH; 7.75, 1H, s, NHNH; 8.19, 1H, m, NHCH_3 . ^{13}C NMR: δ 16.90, 3- CH_3 ; 24.0, 5- CH_3 ; 31.0, NHCH_3 ; 31.50, NHCH_3 ; 47.60, CH_2 ; 85.0, C_5 ; 155.0, C_3 ; 165.61, $\text{C}=\text{S}$; 183.85, $\text{C}=\text{S}$. MS: m/z 273 = $[\text{H}_2\text{L}^1 - \text{H}^+]$.

H_2L^2 . As per general procedure above except with **1** (2.19 g, 9.76 mmol) and 4-ethyl-3-thiosemicarbazide (2.34 g, 19.63 mmol). H_2L^2 was isolated as a white powder (1.32 g, 4.37 mmol, 44%) (Found: C, 43.6; H, 7.3; N, 27.7. Calc. for $\text{C}_{11}\text{H}_{22}\text{N}_6\text{S}_2$: C, 43.7; H, 7.3; N, 27.8%). ^1H NMR (DMSO- d_6): δ 1.05, 6H, m, CH_2CH_3 ; 1.74, 3H, s, 5- CH_3 ; 1.95, 3H, s, 3- CH_3 ; 2.81, 2H, AB quartet, CH_2 ; 3.44, 4H, m, CH_2CH_3 ; 6.25, 1H, s, 5-NH; 7.71, 1H, NHNH; 8.15, 8.25, 2H, t, NHCH_2CH_3 . ^{13}C NMR: δ 15.1, 15.2, CH_2CH_3 ; 16.5, 3- CH_3 ; 24.2, 5- CH_3 ; 38.4, 38.8, CH_2CH_3 ; 47.7, CH_2 ; 85.1, C_5 ; 155.0, C_3 ; 174.4, 182.4, $\text{C}=\text{S}$. MS: m/z 302 = H_2L^2 . Crystals suitable for single crystal X-ray crystallography were grown by slow evaporation of an EtOH–diethyl ether solution.

H_2L^3 . *Method 1.* As per general procedure except with **1** (2.39 g, 10.65 mmol) and 4-phenyl-3-thiosemicarbazide (3.56 g, 21.29 mmol). H_2L^3 was isolated as a white powder (2.43 g, 6.10 mmol, 57%). Elemental analysis results were not consistent with the calculated formula $\text{C}_{19}\text{H}_{22}\text{N}_6\text{S}_2$ due to some *N,N*-diphenyl-[1,3,4]thiadiazole-2,5-diamine being formed as a by-product. The product obtained was of sufficient purity to synthesise metal complexes. MS: m/z 399 = $[\text{H}_2\text{L}^3 - \text{H}^+]$.

N,N-Diphenyl[1,3,4]thiadiazole-2,5-diamine. ^1H NMR (DMSO- d_6): δ 6.94, 2H, m, Ar; 7.31, 4H, m, Ar; 7.57, 4H, m, Ar; 9.91, H, s, NH. ^{13}C NMR: δ 116.8, Ar; 121.0, Ar; 129.0, Ar; 141.1, Ar; 155.7, $\text{C}=\text{N}$. MS: m/z 267 = $[\text{product} - \text{H}^+]$.

Method 2. As per general procedure except with **1** (1.80 g, 8.02 mmol) and 4-phenyl-3-thiosemicarbazide (2.68 g, 16.0 mmol) without adding sulfuric acid. H_2L^3 was isolated as a white powder (1.87 g, 4.68 mmol, 58%) (Found C, 56.2; H, 5.4; N, 20.9. Calc. for $\text{C}_{19}\text{H}_{22}\text{N}_6\text{S}_2 \cdot 0.5\text{H}_2\text{O}$: C, 56.0; H, 5.7; N, 20.6%). ^1H NMR (DMSO- d_6): δ 1.92, 3H, s, 5- CH_3 ; 2.06, 3H, s, 3- CH_3 ; 3.06, 2H, AB quartet, CH_2 ; 6.67, 1H, s, 5-NH; 7.11–7.60, 10H, m, Ar; 8.93, 1H, s, NHNH; 9.74, 1H, s, NHPh ; 9.94, 1H, s, NHPh . ^{13}C NMR: δ 15.8, 3- CH_3 ; 23.7, 5- CH_3 ; 47.3, CH_2 ; 84.6, C_5 ; 124.7–139.0, Ar; 155.2, C_3 ; 173.2, 181.0, $\text{C}=\text{S}$.

Synthesis of complexes

$[\text{Cu}(\text{L}^1)]$. H_2L^1 (0.60 g, 2.19 mmol) and copper acetate (0.44 g, 2.20 mmol) were added to methanol (20 mL). The mixture was heated at reflux for 2 h under an atmosphere of nitrogen and allowed to cool slowly to room temperature. Small dark brown crystals and a brown powder formed which were collected by filtration, washed with diethyl ether and dried *in vacuo* to give $[\text{Cu}(\text{L}^1)]$ as dark brown crystals and a brown powder (2.23 g, 8.14 mmol, 74%) (Found C, 31.3; H, 4.5; N, 24.1. Calc. for $\text{C}_9\text{H}_{14}\text{N}_6\text{S}_2\text{OCu}$: C, 30.9; H, 4.0; N, 24.0%). UV-VIS: λ/nm ($\epsilon/\text{M}^{-1}\text{cm}^{-1}$): 293 (17200), 318 (14800), 417 (6600), 555 (1200), 778 (1400). After 15 h exposure to air: 283 (19200), 314 (16200), 378 (8000), 417 (6240), 483 (2200), 778 (400). MS: m/z 335 = $\{[\text{Cu}(\text{L}^1)] + \text{H}^+\}$. Crystals suitable for single crystal X-ray crystallography were isolated from the reaction mixture.

$[\text{Cu}(\text{L}^2)]$. As per general procedure above except with H_2L^2 (0.40 g, 1.32 mmol) and copper acetate (0.26 g, 1.30 mmol). $[\text{Cu}(\text{L}^2)]$ was isolated as a brown powder (0.14 g, 0.38 mmol, 29%)

(Found C, 36.1; H, 5.6; N, 22.6. Calc. for $\text{C}_{11}\text{H}_{20}\text{N}_6\text{S}_2\text{Cu}$: C, 36.3; H, 5.5; N, 23.1%). MS: m/z 376 = $\{[\text{Cu}(\text{L}^2)] - \text{H}^+\}$.

$[\text{Cu}(\text{L}^3)]$. *Method 1.* As per general procedure except with H_2L^3 (0.069 g, 0.17 mmol) and copper acetate (0.034 g, 0.17 mmol). $[\text{Cu}(\text{L}^3)]$ was isolated as a green/brown powder (0.056 g, 0.12 mmol, 71%). Elemental analysis results were not consistent with the calculated formula $\text{C}_{19}\text{H}_{20}\text{N}_6\text{S}_2\text{Cu}$ due to some *N,N*-diphenyl[1,3,4]thiadiazole-2,5-diamine contamination. MS: m/z 459 = $\{[\text{Cu}(\text{L}^3)] + \text{H}^+\}$.

Method 2. As per general procedure except with H_2L^3 (from ligand method 2) (0.40 g, 1.00 mmol) and copper acetate (0.20 g, 1.00 mmol). $[\text{Cu}(\text{L}^3)]$ was isolated as a dark brown powder (0.35 g, 0.76 mmol, 76%) (Found C, 47.8; H, 3.8; N, 17.4. Calc. for $\text{C}_{19}\text{H}_{20}\text{N}_6\text{S}_2\text{Cu} \cdot \text{H}_2\text{O}$: C, 47.9; H, 4.2; N, 17.6%). MS: m/z 458 = $\{[\text{Cu}(\text{L}^3)] - \text{H}^+\}$.

$[\text{Ni}(\text{L}^1)]$. As per general procedure except with H_2L^1 (0.30 g, 1.09 mmol) and nickel acetate (0.27 g, 1.09 mmol). $[\text{Ni}(\text{L}^1)]$ was isolated as dark-green prismatic crystals (0.13 g, 0.40 mmol, 37%) (Found C, 28.2; H, 5.2; N, 22.2. Calc. for $\text{C}_9\text{H}_{16}\text{N}_6\text{S}_2\text{Ni} \cdot 3\text{H}_2\text{O}$: C, 28.1; H, 5.8; N, 21.8%). ^1H NMR (DMSO- d_6): δ 1.91, 3H, s, CH_3 ; 2.16, 3H, s, CH_3 ; 2.63, 6H, m, NHCH_3 ; 3.28, 2H, s, CH_2 ; 6.85, H, m, NH; 8.0, H, m, NH. ^{13}C NMR: δ 21.5, 22.9, CH_3 ; 27.3, 30.8, NHCH_3 ; 39.5, CH_2 (obscured by solvent peak); 151.1, 157.8, $\text{C}=\text{N}$; 173.3, 176.2, $\text{C}-\text{S}$. MS: m/z 331 = $\{[\text{Cu}(\text{L}^1)] + \text{H}^+\}$. Crystals suitable for single crystal X-ray crystallography were isolated from the reaction mixture.

$[\text{Ni}(\text{L}^2)]$. As per general procedure except with H_2L^2 (1.15 g, 0.50 mmol) and nickel acetate (0.12 g, 0.48 mmol). $[\text{Ni}(\text{L}^2)]$ was isolated as a pink microcrystalline solid (0.11 g, 0.30 mmol, 62%) (Found C, 36.7; H, 5.5; N, 23.2. Calc. for $\text{C}_{11}\text{H}_{20}\text{N}_6\text{S}_2\text{Ni}$: C, 36.8; H, 5.6; N, 23.4%). ^1H NMR (DMSO- d_6): δ 1.03, 6H, m, CH_2CH_3 ; 2.11, 6H, s, CH_3 ; 3.12, 4H, m, CH_2CH_3 ; 4.02, 2H, s, CH_2 ; 6.94, 2H, m, NHCH_2CH_3 . ^{13}C NMR: δ 14.4, CH_2CH_3 ; 20.4, CH_3 ; 39.5, CH_2CH_3 ; 46.2, CH_2 ; 156.9, $\text{C}=\text{N}$; 171.0, $\text{C}-\text{S}$. MS: m/z 359 = $\{[\text{Ni}(\text{L}^2)] + \text{H}^+\}$. Crystals suitable for single crystal X-ray crystallography were grown by slow evaporation of a methanol solution. These were analysed as the oxidised complex $[\text{Ni}(\text{L}^2\text{O})]$.

$[\text{Ni}(\text{L}^3)]$. *Method 1.* As per general procedure except with H_2L^3 (1.06 g, 2.66 mmol) and nickel acetate (0.66 g, 2.66 mmol). $[\text{Ni}(\text{L}^3)]$ was isolated as a green/brown powder (1.07 g, 2.35 mmol, 88%). Elemental analysis results were not consistent with the calculated formula $\text{C}_{19}\text{H}_{20}\text{N}_6\text{S}_2\text{Ni}$ due to some *N,N*-diphenyl[1,3,4]thiadiazole-2,5-diamine contamination. ^1H NMR (DMSO- d_6): δ 2.09, 3H, s, CH_3 ; 2.33, 3H, s, CH_3 ; 3.54, 2H, s, CH_2 ; 6.90–7.58, 10H, m, Ar; 9.42, H, s, NH; 10.18, H, s, NH. ^{13}C NMR: δ 23.0, CH_3 ; 23.6, CH_3 ; 39.5, CH_2 (obscured by solvent peak); 118.3–141.0, Ar; 153.8, 162.3, $\text{C}=\text{N}$; 169.4, 173.2, $\text{C}-\text{S}$. MS: m/z 455 = $\{[\text{Ni}(\text{L}^3)] + \text{H}^+\}$. Crystals suitable for single crystal X-ray crystallography were grown by slow evaporation of a dichloromethane solution.

Method 2. As per general procedure except with H_2L^3 (from ligand method 2) (0.40 g, 1.00 mmol) and nickel acetate (0.25 g, 1.00 mmol). $[\text{Ni}(\text{L}^3)]$ was isolated as a light brown powder (0.37 g, 0.81 mmol, 81%) (Found C, 48.7; H, 4.5; N, 17.4. Calc. for $\text{C}_{19}\text{H}_{20}\text{N}_6\text{S}_2\text{Ni} \cdot \text{H}_2\text{O}$: C, 48.4; H, 4.3; N, 17.8%). NMR results were similar to method 1. MS: m/z 455 = $\{[\text{Ni}(\text{L}^3)] + \text{H}^+\}$.

Serum stability studies

Stock solutions of blank samples $\text{Cu}(\text{OAc})_2$ and $\text{Cu}(\text{hist})_2$ and the test sample $[\text{Cu}(\text{L}^1\text{O})]$ ($5.1 \times 10^{-2}\text{ mol L}^{-1}$) were made up in DMSO solution. The stock solutions (0.125 mL) were added to 2.5 mL of human serum and the samples were incubated in a thermostated oil bath at 37 °C for 6 h before being chromatographed. The PD-10 (Sephadex G-25) size exclusion columns were equilibrated with 25 mL of 0.01 M KH_2PO_4 buffer prior to use. The columns were

eluted with 0.01 mol L⁻¹ KH₂PO₄. Three fractions (ca. 2 mL each) were collected and the protein containing fractions were identified by their absorbance at 280 nm. The fractions were diluted to 25 mL with phosphate buffer solution and the copper concentrations were determined by ICP-AES. The total copper concentration in the diluted fractions was expected to be 16 ppm. The first and second fractions were found to be the major protein-containing fractions by their high intensity absorption in the UV spectrum at 280 nm. The copper concentrations measured in the fractions collected were: Cu(OAc)₂ 1: 2.4 ppm, 2: 3.1 ppm; Cu(hist)₂ 1: 2.5 ppm, 2: 7.7 ppm CuL¹O 1: 0.12 ppm, 2: 0.09 ppm (background level).

X-Ray crystallography

Crystals were mounted on a glass fibre using perfluoropolyether oil and cooled rapidly to 150 K in a stream of cold N₂ using an Oxford Cryosystems CRYOSTREAM unit. Diffraction data were measured using an Enraf-Nonius KappaCCD diffractometer (graphite-monochromated Mo-K α radiation, $\lambda = 0.71073$ Å). Intensity data were processed using the DENZO-SMN package.³⁴

The structures were solved using the direct-methods program SIR92,³⁵ which located all non-hydrogen atoms. Subsequent full-matrix least-squares refinement was carried out using the CRYSTALS program suite.³⁶

CCDC reference numbers 237483–237488.

See <http://www.rsc.org/suppdata/dt/b4/b406429a/> for crystallographic data in CIF or other electronic format.

H₂L². The structure was solved in the space group $P\bar{1}$ using the direct-methods program SIR92,³⁵ which located all non-hydrogen atoms. Coordinates and anisotropic thermal parameters of all non-hydrogen atoms were refined. The NH hydrogen atoms were located in a difference Fourier map and their coordinates and isotropic thermal parameters were subsequently refined. Other hydrogen atoms were positioned geometrically after each cycle of refinement. A three-term Chebychev polynomial weighting scheme was applied. Refinement converged satisfactorily to give $R = 0.0340$, $wR = 0.0374$.

[Cu(L¹)]. The structure was solved in the space group $P\bar{1}$ using the direct-methods program SIR92,³⁵ which located all non-hydrogen atoms. Coordinates and anisotropic thermal parameters of all non-hydrogen atoms were refined. The NH and OH hydrogen atoms were located in a difference Fourier map and their coordinates and isotropic thermal parameters subsequently refined. Other hydrogen atoms were positioned geometrically after each cycle of refinement. A three-term Chebychev polynomial weighting scheme was applied. Refinement converged satisfactorily to give $R = 0.0277$, $wR = 0.0351$.

2. Examination of the systematic absences of the intensity data showed the space group to be either Pc or $P2_1/c$. The structure could not be solved in the latter space group but was solved in the space group Pc using the direct-methods program SIR92,³⁵ which located all non-hydrogen atoms. Examination of the resulting model showed no additional symmetry elements to be present. Coordinates and anisotropic thermal parameters of all non-hydrogen atoms were refined. The NH hydrogen atoms were located in a difference Fourier map and their coordinates and isotropic thermal parameters were subsequently refined. Other hydrogen atoms were positioned geometrically after each cycle of refinement. The relative contribution of the two twin components to overlapping reflections was included as a parameter in the refinement. A four-term Chebychev polynomial weighting scheme was applied. Refinement converged satisfactorily to give $R = 0.413$, $wR = 0.0480$.

[Ni(L¹)]. Examination of the systematic absences of the intensity data showed the space group to be $Pbca$. Coordinates and anisotropic thermal parameters of all non-hydrogen atoms were refined. The NH hydrogen atoms were located in a difference Fourier map and their coordinates and isotropic thermal parameters subsequently refined. Other hydrogen atoms were positioned geometrically after

each cycle of refinement. A three-term Chebychev polynomial weighting scheme was applied. Refinement converged satisfactorily to give $R = 0.0266$, $wR = 0.0316$.

[Ni(L³)]. Examination of the systematic absences of the intensity data showed the space group to be $P2_1/c$. Coordinates and anisotropic thermal parameters of all non-hydrogen atoms were refined. The NH hydrogen atoms were located in a difference Fourier map and their coordinates and isotropic thermal parameters subsequently refined. Other hydrogen atoms were positioned geometrically after each cycle of refinement. A three-term Chebychev polynomial weighting scheme was applied. Refinement converged satisfactorily to give $R = 0.0291$, $wR = 0.0310$.

[Ni(L²O)]. Examination of the systematic absences of the intensity data showed the space group to be $P2_1/c$. Coordinates and anisotropic thermal parameters of all non-hydrogen atoms were refined. The thermal parameters of the C atoms of one of the ethyl groups were seen to be excessively large and anisotropic, indicative of disorder. This was modelled as disorder over two orientations. The coordinates, anisotropic thermal parameters and site occupancies of the disordered C atoms were refined. Geometric restraints were applied: the N–C bonds were restrained to be 1.47(2) Å long; the C–C bonds to 1.54(2) Å and the N–C–C angles to 110(2)°. Similarity restraints have been applied to the components of the atomic displacement parameters of directly bonded N and C atoms parallel to their bonds. The NH hydrogen atoms were located in a difference Fourier map and their coordinates and isotropic thermal parameters subsequently refined. Other hydrogen atoms were positioned geometrically after each cycle of refinement. The difference Fourier map suggested that the ‘backbone’ methyl groups were disordered and their hydrogen atoms were placed at positions corresponding to the idealised geometry of the predominant orientation. A three-term Chebychev polynomial weighting scheme was applied. Refinement converged satisfactorily to give $R = 0.0334$, $wR = 0.0335$.

Acknowledgements

We thank EPSRC for funding a postdoctoral fellowship (P.S.D) and GSK for financial support and funding a D. Phil scholarship (J. M. H.).

References

- D. X. West, S. B. Padhye and P. B. Sonawane, *Struct. Bonding (Berlin)*, 1991, **76**, 1.
- D. H. Petering, *Bioinorg. Chem.*, 1972, **1**, 255.
- D. X. West, A. E. Liberta, S. B. Padhye, R. C. Chikate, P. B. Sonawane, A. S. Kumbhar and R. G. Yerande, *Coord. Chem. Rev.*, 1993, **123**, 49.
- K. Wada, Y. Fujibayashi and A. Yokoyama, *Arch. Biochem. Biophys.*, 1994, **310**, 1.
- Y. Fujibayashi, H. Taniuchi, Y. Yonekura, H. Ohtani, J. Konishi and A. Yokoyama, *J. Nucl. Med.*, 1997, **38**, 1155.
- J. L. J. Dearling, J. S. Lewis, D. W. McCarthy, M. J. Welch and P. J. Blower, *J. Chem. Commun.*, 1998, 2531.
- Y. Fujibayashi, C. S. Cutler, C. J. Anderson, D. W. McCarthy, L. A. Jones, T. Sharp, Y. Yonekura and M. J. Welch, *Nucl. Med. Biol.*, 1999, **26**, 117.
- J. S. Lewis, R. Laforest, T. L. Buettner, S.-K. Song, Y. Fujibayashi, J. M. Connet and M. J. Welch, *Proc. Natl. Acad. Sci. USA*, 2001, **98**, 1206.
- J. S. Lewis, T. L. Sharp, R. Laforest, Y. Fujibayashi and M. J. Welch, *J. Nucl. Med.*, 2001, **42**, 655.
- J. L. J. Dearling, J. S. Lewis, G. D. Mullen, M. J. Welch and P. J. Blower, *J. Biol. Inorg. Chem.*, 2002, **7**, 249.
- A. R. Cowley, J. R. Dilworth, P. S. Donnelly, E. Labisbal and A. Sousa, *J. Am. Chem. Soc.*, 2002, **124**, 5270.
- J. R. Ballinger, *Semin. Nucl. Med.*, 2001, **XXXI**, 1.
- P. J. Blower, J. S. Lewis and J. Zweit, *Nucl. Med. Biol.*, 1996, **23**, 957.
- M. A. Green, D. L. Klippenstein and J. R. Tennison, *J. Nucl. Med.*, 1988, **29**, 1549.
- C. J. Anderson and M. J. Welch, *Chem. Rev.*, 1999, **99**, 2219.
- V. M. Leovac, V. I. Češljević, G. Argay, A. Kálmán and B. Ribár, *J. Coord. Chem.*, 1995, **34**, 357.
- S. C. Davies, M. C. Durrant, D. L. Hughes, A. Pezeshk and R. L. Richards, *J. Chem. Res. (S)*, 2001, 100.

- 18 Y. Arano, M. Yabuki, T. Yahata, K. Horiuchi and A. Yokoyama, *Chem. Pharm. Bull.*, 1990, **38**, 3099.
- 19 Y. Arano, M. Yabuki, A. G. Jones and A. Yokoyama, *Chem. Pharm. Bull.*, 1991, **39**, 104.
- 20 D. H. Hunter, C. McRoberts and J. J. Vittal, *Can. J. Chem.*, 1998, **76**, 522.
- 21 C. N. O'Callaghan and D. Twomey, *J. Chem. Soc.*, 1967, **22**, 2400.
- 22 B. Stanovnik and M. Tišler, *J. Org. Chem.*, 1961, **26**, 5200.
- 23 P. J. Blower, T. C. Castle, A. R. Cowley, J. R. Dilworth, P. S. Donnelly, E. Labisbal, F. E. Sowrey, S. J. Teat and M. J. Went, *Dalton Trans.*, 2003, 4416.
- 24 E. Bermejo, A. Castiñeiras, L. J. Ackerman, M. D. Owens and D. X. West, *Z. Anorg. Allg. Chem.*, 2001, **627**, 1966.
- 25 G. J. Colpas, M. Kumar, R. O. Day and M. J. Maroney, *Inorg. Chem.*, 1990, 4779.
- 26 M. E. Padilla-Tosta, D. Fox, M. G. B. Drew and P. D. Beer, *Angew. Chem.*, 2001, **40**, 4235.
- 27 V. B. Arion, N. V. Gerbeleu and K. M. Indrichan, *Russ. J. Inorg. Chem.*, 1985, **30**, 70.
- 28 S. Yokota, Y. Tachi and S. Itoh, *Inorg. Chem.*, 2002, **41**, 1342.
- 29 R. I. Maurer, P. J. Blower, J. R. Dilworth, C. A. Reynolds, Y. Zheng and G. D. Mullen, *J. Med. Chem.*, 2002, **45**, 1420.
- 30 A. R. Cowley, J. R. Dilworth, P. S. Donnelly, E. Labisbal and A. Sousa, *J. Am. Chem. Soc.*, 2002, **124**, 5270.
- 31 C. J. Mathias, S. R. Bergmann and M. A. Green, *J. Nucl. Med.*, 1995, **36**, 1451.
- 32 J. Masuoka and P. Saltman, *J. Biol. Chem.*, 1994, **41**, 25557.
- 33 J. R. Ballinger, J. R. Dilworth, P. S. Donnelly and J. M. Heslop, 2003, unpublished results.
- 34 Z. Otwinowski and W. Minor, *Methods Enzymol.*, 1997, **276**, 307.
- 35 A. Altomare, G. Cascarano, G. Giacovazzo, A. Guagliardi, M. C. Burla, G. Polidori and M. Camalli, *J. Appl. Crystallogr.*, 1994, **27**, 435.
- 36 D. J. Watkin, C. K. Prout, J. R. Carruthers, P. W. Betteridge and R. I. Cooper, in *CRYSTALS issue 11*, Oxford, UK, 2001.